



## Seismic Performance of Box Girder Bridge with Non-Linear Static Pushover Analysis

Nilanjan Tarafder<sup>1</sup> and L.V. Prasad M.<sup>2</sup>

<sup>1</sup>Research Scholar, Civil Engineering Department,  
National Institute of Technology, Silchar-788010 (Assam), India.

<sup>2</sup>Assistant professor, Civil Engineering Department,  
National Institute of Technology, Silchar-788010 (Assam), India.

(Corresponding author: Nilanjan Tarafder)

Received 16 January 2020, Revised 18 March 2020, Accepted 20 March 2020)

(Published by Research Trend, Website: [www.researchtrend.net](http://www.researchtrend.net))

**ABSTRACT:** Herein, a box girder bridge, prepared using self-compacting concrete (SCC), is studied to understand its behaviour during an earthquake. The bridge under consideration was constructed by PWD, Silchar with normal M40 grade concrete. The concrete type is ancient for the structure category at present and there is need for a new concrete material to be used which will improve the performance of bridges. In our present endeavour, practically used concrete was replaced with new SCC to examine the performance using pushover analysis. For this, a three dimensional finite element model was prepared and all the load combinations were evaluated including critical load case. For seismic investigation, pushover analysis was performed with respect to the Indian Standard response spectrum to examine the displacement pattern, base shear capacity and demand-capacity behaviour of the bridge piers in longitudinal and transverse direction. The results shows that performance of the bridge is enhanced in both the directions including 16 improved drift values and demand capacity ratio also found to be within the prescribed limit. The proposed new material, SCC, improved the performance of the bridge in both longitudinal and transverse directions.

**Keywords:** Bridge structure, Pushover Analysis, Base Shear, Capacity Curve, Demand-Capacity Ratio, Drift.

**Abbreviations:** SCC, self compacting concrete; SMA, shape memory alloy; 3D, three dimensional; FE, finite element; RC, reinforced concrete; RCC, reinforced cement concrete; PWD, public works department; PHE, public health engineering; PSC, pre stressed concrete; BOBJ, bridge object; IRC, Indian road congress; IS, Indian standard; ACI, American concrete institute; AASTHO LFRD, American association of state highway and transportation officials - load and resistance factor design; D/C, design capacity; LG, longitudinal; TR, transverse; B, bent cap section; Long, longitudinal direction; Trans, transverse direction; BaseX, base shear for longitudinal direction; BaseY, base shear for transverse direction; Disp.X, displacement in longitudinal direction; Disp.Y, displacement in transverse direction.

### I. INTRODUCTION

Any structure is a state of the art of human understanding about the material applications. A bridge is an essential structure for efficient connection between two parts divided by river or some ground obstructions. It provides connection between two parts over a water body or those of a city by dividing the traffic jam in the bridge lane and ground level roadway. With time, bridge design became increasingly complicated due to the desire to provide functionality to cover very long distance with an aesthetic appeal. Every structure is mainly prone to sudden natural calamities. Hence, it is very important to safeguard the exquisite structure from any natural calamity to ensure safety of life and economy of the country. Various studies are carried out to improve the structure and enhance its resistance against earthquake and wind forces. An innovative type of concrete called Self-compacting concrete, is thought to be suitable in order to improve the performance of bridge structure under these forces. This type of concrete can flow freely without any vibrational force and fill the gaps of any type of congested reinforcement in no time.

To study the effects of ground motion duration from subduction earthquakes Lopez *et al.*, conducted an experiment and studied the effects on the performance of RC bridge columns. Even though similar deformation levels was achieved, subduction ground motions damaged the specimens more compared to crustal

motions. Their results showed that subduction ground motions imposed greater material strains leading to buckling of reinforcement bar which was not reached under similar circumstances from crustal ground waves [1]. To limit the superstructure displacement Ghosh *et al.*, (2011) used 4 different types of protection devices during an earthquake- yielding stopper device, rigid stopper device, superelastic shape memory alloy (SMA) restrainer and steel restrainer. In order to prevent bearing failure, all the protection devices had comparable performance during an earthquake. The SMA restrainer showed marginally greater pier/abutment forces with improved energy dissipation and added protection against greater ground shaking stages due to strain hardening at upper strain levels [2]. Another research was done by Kulkarni *et al.*, (2016) to inspect the response reduction factors' applicability, as per seismic design codes, for the bridges having tall piers. As per their results, P-D effects are very important for tall piers, even when the moment of P-D was low comparing with the capacity due to plastic moment. The ductility capacity of hollow piers was 8 as per pushover analysis results [3]. Priestley and Seible (1996) proved that, concrete strains due to compression in plastic hinge area surpassed the unconfined compression strain and spalling of concrete cover took place at a displacement ductility level 2 to 3. According to them, it is avoidable with the confinement of close-spaced transverse hoops or spirals, or else crushing quickly spreads in to the core, leading to buckling of

longitudinal reinforcement and rapid strength degradation, resulting in inability to support gravity load [4]. Mohammed (2016) tried to quantify the effect of duration on collapse capacity and to recommend whether this effect should be included in seismic design provisions. His study showed that spectral accelerations at collapse for columns subjected to long-duration motions were lower by 21% to 29% than the column subjected to short duration motion. The geometric mean of the displacement capacities of the long-duration specimens was 32% lower than the maximum displacement capacity of the short-duration specimen [5]. Earlier, research has revealed that reinforcement bars are prone to buckling under tensile strain. In order to quantify this effect Feng *et al.*, (2015) developed a hybrid analysis method to assess the effect of seismic load on buckling of reinforcement bars. A fibre-based model was prepared to conduct nonlinear time history analysis for 40 earthquake ground motions. They also conducted a parametric study to develop design equations which will deliver strain restrictions before the bar buckles [6]. Whereas Goodnight *et al.*, (2013) did an experimental study on 30 circular, well-confined, bridge columns with variable lateral displacement history, transverse reinforcement, axial load, aspect ratio and longitudinal steel to assess the performance of them 8 of the columns having similar geometry and detailing were exposed to numerous unidirectional displacements as well as cyclic loading. Their results showed that load history influenced the buckling of the reinforcement bar but the strain displacement relationship of cyclic loading was not influenced along the envelope curve [7]. A research program was undertaken by Lehman *et al.*, (2004) to evaluate the seismic performance of well-confined circular RC bridge columns at some damage state range. The deciding variables were axial load ratio, longitudinal reinforcement ratio, aspect ratio, spiral reinforcement ratio, and well-confined region length next to the plastic hinging zone. Using cumulative probability curves they concluded that the key damage states of residual cracking, core crushing and cover spalling were related to concrete compressive strain and longitudinal reinforcement tensile strain [8]. 3D continuum-based FE simulation was executed by Babazadeh *et al.*, (2015) to analyse flexure-dominated ductile RC bridge columns for evaluating intermediate damage limit states. Results were compared and validated with 4 large-scale experimental results. Depending on the simulation results, intermediate damage limit states were determined by applying the validated models [9]. Damage control curvature relationship and dimensionless serviceability was developed by Kowalsky (2000) by moment-curvature analysis of circular bridge columns. The outputs were subjected to only on the section diameter and column axial load ratio. The relationships were used to evaluate displacement ductility, curvature, equivalent viscous damping capacities and drift ratio for the considered design limit states [10]. To pretend the damage development procedure of RC bridge piers, Su *et al.*, (2017) adopted a fiber beam-column section with earthquake and quasi-static loads considering longitudinal bars' low-cycle fatigue and buckling. Damage of concrete cover was calculated with the tensile strain. Results showed that the damage index reflected the damage states at the onset of spalling, bar buckling, significant spalling and failure [11]. An experimental study was conducted by Meesaraganda and Tarafder (2019) on self-compacting concrete to understand its property and long term

effects. It is a type of concrete which is flowable under its own weight without any requirement of vibration and this property will be very profitable in the construction of congested type of reinforcements. The concrete was also proved to be durable in long term effects including resistance against acid attacks in cities near water [12]. Literature review shows that various studies were done on the displacement limitations and behaviour of structural element considering normal concrete which is presently used for construction. A new concrete type can be implemented for construction of bridges which may improve the performance. So a study was conducted using new self compacting concrete as material type and structure behaviour against earthquake was analysed using pushover analysis. In this paper, a bridge structure over the "Barak" river in Silchar, India was studied. The project was handled by the Public Works Department (PWD), Assam. Silchar is situated in the earthquake zone V and the area is having soil type III. This is a very weak combination for building any structure. So the self-compacting concrete concept is used in this study to strengthen the structure. The main advantage of the proposed system is, gaining high strength comparing with same grade of normal concrete, removal of external vibration for construction leading to energy saving and easy pouring of concrete mixture in the heavily congested reinforcements of bridge pier [13]. The manuscript concentrates on the base shear capacity, demand capacity ratio and drift of the bridge piers. All the analysis were done under severe seismic activity and with heavy traffic load on the bridge structure. The demand capacity ratio was evaluated, for the type of bridge selected, which have not been studied with the proposed material. The studied bridge was analysed with the help of "CSiBridge" software. The paper clearly demonstrates the behaviour of the bridge under seismic loading. The site under evaluation is mainly prone to seismic actions, therefore study was carried out to counteract this action. The study shows that, constructed bridge is able to resist any magnitude of earthquake which came in the past in this region.

## II. CONCRETE PROPERTY

Self-compacting concrete was used in this study as input parameter of concrete type. The mix proportion of preparing SCC is provided in Table 1 with detailed ingredients. The properties of fresh and hardened concrete was also available from the previous study of the authors and provided in Table 2.

## III. BRIDGE DESIGN CONSIDERATIONS

Bridge under consideration is located over Barak River on the eastern side of Silchar town in Assam. The approach on Silchar town side is connected to the road behind Public Health Engineering (PHE) Department campus boundary. The approach on the airport side was proposed abutting the boundary of the Newspaper office and connected to the existing road alignment. Silchar comes under the earthquake zone V which is categorised as severe and soil zone type III which is poorly graded sandy and clayey soil. The bridge was designed and constructed considering the fact of high earthquake-prone area and poor soil type region. The construction project was completed by Public Works Department (PWD). Flood level studies were done before designing the bridge so that the flood level in monsoon season does not block any uses of the bridge. The formation levels by PWD are shown in Table 3.

**Table 1: Mix proportion for M40 grade SCC [12].**

Cement (Kg)	Fly ash (Kg)	Coarse aggregate (Kg)	Fine aggregate (Kg)	Water (Lit.)	Super plasticizer (%)	Viscosity modifying agent (%)
425	147	707	944	193	1.40	0.20

**Table 2: Properties of fresh and hardened state of SCC [12].**

Slump cone test		V-funnel test		L box test			EFNARC specification	Compressive strength (MPa)
H-flow (mm)	T50 (sec)	Time for concrete discharge (sec)	T5 (sec)	Time for 0-200 mm spread (sec)	Time for 0-200 mm spread (sec)	H <sub>2</sub> /H <sub>1</sub>		
720	4.52	10.00	12.50	3.80	6.00	0.95	Satisfied	49.24

**Table 3: Different levels of bridge structure [14].**

Type	Formation level (m)
Formation level	105
High flood level	99.95
Lowest bed level	100
Ground level	100
Design discharge	97.70
Top of abutment	102.20
Bottom of abutment	97.20
Top of bent cap	97
Bottom of bent cap	94.75

**A. Structural Parameters**

The spans of the bridge were constructed by balanced cantilever method. Length of the central span was 122.725 m and each of the both shore span lengths were 65 m. Overall width of the bridge section, also known as the bridge deck section width was 12 m. The carriageway widths and the width of the footpath were 8.5 m and 1.5 m respectively. The depth of box girder section of the bridge was varying parametrically from 2.5 m to 7.7 m throughout abutment portion to the pier section of the bridge length.

**B. Analytical Input Parameters**

The bridge was analysed with the help of the software "CSiBridge". With the proposed software, engineers can simply define complex bridge geometries, load cases and boundary conditions. The bridge models were defined parametrically using known terms to bridge engineers like- spans, layout lines, abutments, bearings, bent caps etc. It allows easy selection of vehicles and application of vehicle loads over the bridge deck. CSiBridge is also capable of analysing and designing of concrete or steel bridge structures under any load combinations applied.

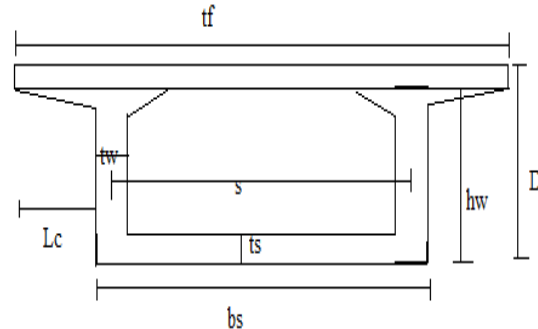


**Fig. 1. Cross section of bridge deck.**

A detailed cross section of bridge deck is shown in Fig. 1. It is visible from cross section diagram that the bridge under study is a Box Girder bridge. Modelling of the bridge deck section was done as per the PWD bridge geometry. Detailed measurements of deck section is shown in Table 4. The section includes top flange thickness, top slab thickness, bottom slab thickness, overall depth of deck, web thickness, web height, cantilever thickness and length. Other parts of the bridge like- abutment, bent cap, column, concrete property, steel type provided etc. were considered as per the PWD guidelines for this bridge. Table 5 shows the measurements for abutment, bent cap and column sections. Self-compacting concrete and steel property were described in Table 6 (a) and (b). The grade of concrete and steel used in the construction was M40 and Fe-500 respectively. There are six spans in the bridge and two types of bearing conditions were used. Table 7 shows the span details of bearing property used in the bridge structure and elevation as well as bearing angle in the respective sections of bridge.

**Table 4: Details of bridge deck section [14].**

Component	At abutment section	At pier section
	Length (m)	Length (m)
Top flange (t <sub>f</sub> )	12	12
Overall depth (D)	2.5	7.7
Top slab thickness (t <sub>t</sub> )	0.535	0.96
Bottom slab thickness (t <sub>s</sub> )	0.275	0.7
Web thickness (t <sub>w</sub> )	0.35	0.5
Cantilever (L <sub>c</sub> )	3	3
Cantilever thickness	0.535	0.96
Web to web spacing (S)	5.65	5.5
Web height (h <sub>w</sub> )	1.965	6.740
Soffit width (b <sub>s</sub> )	6	6

**Table 5: Details of bridge components [14].**

Bridge component	Length (m)	Width (m)	Height (m)
Abutment	12	2.5	5
Bent cap	4.5	4.5	4.5
Pier	4.5	0.8	9.5

**Table 6(a): Details of material property-1.**

Item	Grade
Pier	M40 self compacting concrete
PSC box girder	M40 self compacting concrete
Structural steel	Fe 500

**Table 6(b): Details of material's mechanical property-2.**

Material	Unit weight (kN/m <sup>3</sup> )	Unit mass (kN-s <sup>2</sup> /m <sup>4</sup> )	Young's modulus (kN/m <sup>2</sup> )	Shear modulus (kN/m <sup>2</sup> )	Poisson's ratio	Co-efficient of thermal expansion (1/C)
Pier M40 (SCC)	24.993	2.5485	38000000.	15322580.65	0.24	1.9000E-05
PSC box girder M40 (SCC)	24.993	2.5485	38000000.	15322580.65	0.24	1.9000E-05
HYSD 500	76.973	7.8490	200000000.	—	0.3	1.1700E-05
Tendon	76.973	7.8490	206842736.7	—	0	1.1700E-05

**Table 7: Bridge model summary.**

Bridge object	Span name	Station (m)	Type	Bearing property	Bearing elevation (m)	Bearing angle (degrees)
BOBJ1	Start abutment	0.	Abutment	Bearing free	-2.65	0.
BOBJ1	Span 1	62.75	Bent	Bearing fix	-3.2	0.
BOBJ1	Span 2	67.25	Bent	Bearing fix	-3.2	0.
BOBJ1	Span 3	126.3625	Bent	Bearing fix	-7.85	0.
BOBJ1	Span 4	185.475	Bent	Bearing fix	-3.2	0.
BOBJ1	Span 5	189.975	Bent	Bearing fix	-3.2	0.
BOBJ1	Span 6	252.725	Abutment	Bearing free	-2.65	0.

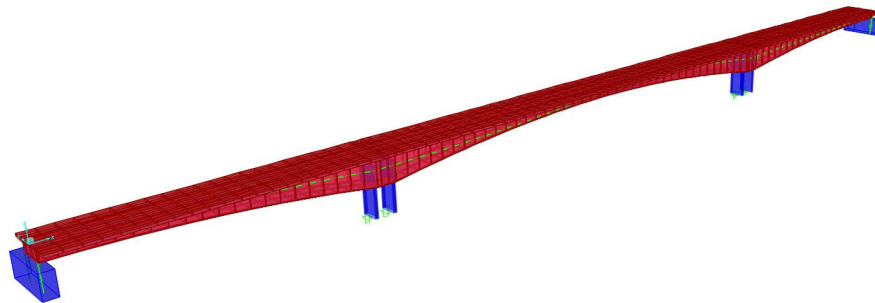


**Fig. 2.** Full bridge section - 3D.

**Table 8: Details of vehicle load applied on the bridge structure.**

Load pattern	Vehicle class	Lane number	Station (m)	Start time (sec)	Direction of vehicle movement	Speed (m/sec)
Truck	IRC A	Lane 1	0.	0.	Forward	35.
Truck	IRC A	Lane 1	0.	0.5	Forward	30.
Truck	IRC A	Lane 2	130.	0.	Backward	35.
Truck	IRC A	Lane 2	130.	0.5	Backward	30.

A 3 dimensional view of the full bridge section was shown in Fig. 2. Here x, y and z are the longitudinal, transverse and vertical direction of the bridge.

**IV. LOADING AND OTHER DESIGN PARAMETERS**

The input loading parameters considered was self-weight of structure, railing load, pedestrian load, wearing coat load, vehicle load and earthquake load. Unit weight considered for reinforced cement concrete (RCC) and Pre-stressed concrete (PSC) was 25 kN/m<sup>3</sup>. The same for wearing coat was considered as 22 kN/m<sup>3</sup>. Load for each railing in the each side of bridge deck was taken as 1 kN/m. Wearing coat loading was 1.5 kN/m over the deck section as pavement. For carriageway live load – Two lanes of IRC Class A loading and footpath live load as 5 kN/m<sup>2</sup> was considered [15]. For earthquake load, response spectrum from IS-1893:2016 was followed. The boundary constraint for the bridge was fixed in all directions. Details of vehicle loads applied on the bridge structure are shown in the Table 8.

**V. ANALYSIS**

The analysis of the bridge object was done by the CSiBridge Run Analysis command. CSiBridge is capable of analysing very complex bridge structure under any loading condition. For each and every different loads and load combinations, analysis was done and the analysis results can be viewed likewise [16, 17]. The response spectrum function used in the pushover analysis was IS-1893:2016 design spectrum function for earthquake zone V and stiff soil which represents Silchar. Seismic design request was generated using AASHTO LRFD 2002 seismic design code for bridges selecting seismic design category D and previously defined response spectrum as a function for pushover analysis [18]. At first dead load of entire structure was applied and several iterations were performed to calculate crack section properties. Based on these crack section properties, response spectrum analysis was performed and lastly pushover analysis was performed.

The response spectra for seismic zone V and proposed area soil type, is shown in the Fig. 3. Response reduction factor was used for RC buildings with special moment resisting frame condition and importance factor was taken as per IS-1893:2016.

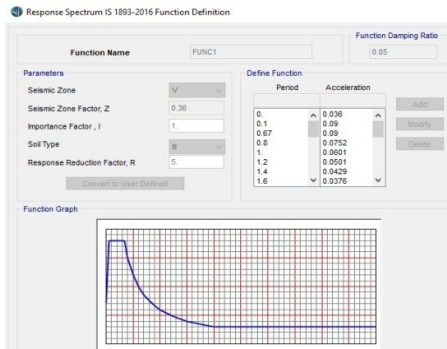


Fig. 3. Response spectrum function.

## VI. RESULT AND DISCUSSION

### A. Capacity Curve

Literature study showed that force-displacement behaviour of a RC bridge column was determined by Babazadeh *et al.*, (2015) they analysed the behaviour irrespective of direction because of the circular column [9]. So here behaviour was studied in both longitudinal and transverse directions. In this study, capacity of the structure was characterised by a base shear-displacement curve obtained by nonlinear static pushover analysis. In this method first a distribution for the lateral loads on the frame was assumed and increased monotonically. Due to this, the structural element yields chronologically and the structure experiences a loss in stiffness. Fig. 4 shows the capacity curve of all the bent cap sections in longitudinal direction. It can be seen from the figure that, Bent 1 and 4 acted similarly under pushover load and the base shear generated in these bent caps was very less compared to that of the bent caps 2 and 3. Whereas bent caps 1 and 4 experienced a shear around 100 kN, bent caps 2 and 3 experienced 770 kN of base shear under the pushover loading. It is because the internal span length was very long which was supported by the bents 2 and 3, compared to the outer span lengths supported by bents 1 and 4. None of the bents reached their yield strength and was within the elastic limit resulting good ductile behaviour in longitudinal direction. Also it is to be noticed that bent 1 and 2 experienced a little initial negative base shear whereas other two bent caps were observed only to have positive base shears. It is because of the type of response spectra used in the study and its effect on the location of the bent cap. Fig. 5 shows the capacity curve of all the bent cap sections in transverse direction. This figure is divided into two parts as in the same plot bent 2 & 3 and bent 1 & 4 were overlapping resulting in trouble reading the graph. It can be seen from the figure that, bent 1 and 4 acted similarly under pushover load and the base shear generated in the bent caps due to the pushover load is very less compared to that of the bent caps 2 and 3. Whereas bent caps 1 and 4 experienced a shear around 500 kN, bent caps 2 and 3 experienced 4800 kN of base shear under the pushover loading. It is because the internal span length was very long which was supported by the bents 2 and 3, compared to the outer span lengths supported by bents 1 and 4. Here bents 1 and 4 did not

reached their yield strength and was within the elastic limit resulting good ductile behaviour in transverse direction. But bents 2 and 3 reached their yield point at base shear values 4800 kN and 4760 kN respectively. At this point the displacement of the two bents was 21.8 mm and 21.6 mm respectively which ultimately reached the final values of 26 mm and 25.8 mm.

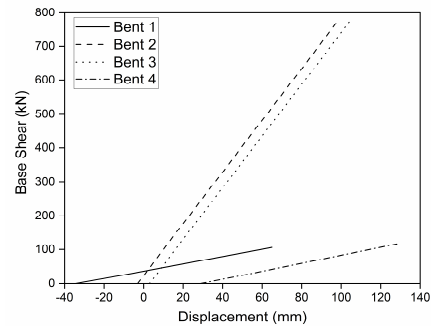


Fig. 4. Capacity curve of bent cap sections in longitudinal direction.

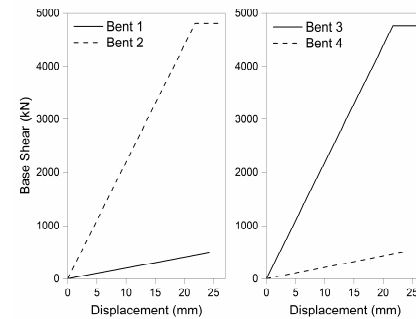


Fig. 5. Capacity curve of bent cap sections in transverse direction.

### B. Demand/Capacity (D/C) Ratio

It is an important aspect to check the seismic vulnerability of bridges when subjected to a seismic event. Demand capacity (D/C) ratio is the ratio between demand of the structure in the specified conditions under all external applied forces and the capacity of the structure which it will perform throughout its life time to resist the external forces. This term is introduced in the study to evaluate the performance of the structure. D/C ratio 0 means no damage to structure and 1 means structure is at the verge of failure. Fig. 6 shows the capacity of the structure as well as the demand as per the pushover load applied in the study. In the graph, BT corresponds to the Bent Cap section. 1, 2, 3 and 4 are respective bent cap sections. LG and TR denotes the longitudinal and transverse directions. As we can see, capacity in both the directions are higher than that of the demand which is recommended for safety of the structure. In longitudinal direction, the capacity of the bent cap section is far more greater than that in transverse direction. Fig. 7 represents the demand to capacity (D/C) ratio for the bridge under study. The minimum and maximum D/C ratio was found to be 0.194 and 0.383 respectively. It was found that, in transverse direction D/C ratio is same for all of the bent cap sections with a value of 0.25. Even the maximum D/C ratio lies within the safe limit of the structure i.e., 1. Hence the bridge is able to resist all the dead, live and moving loads very efficiently and moreover external seismic forces can also be fully taken by the bridge. All

the members of the structure are within the safe limit and no member fails under study. The bridge neither will collapse nor it will have any serious damage under provided circumstances. When the demand to capacity ratio comes out to be less than 1, structure is considered safe but if the ratio found to be more than 1, the structure requires retrofitting.

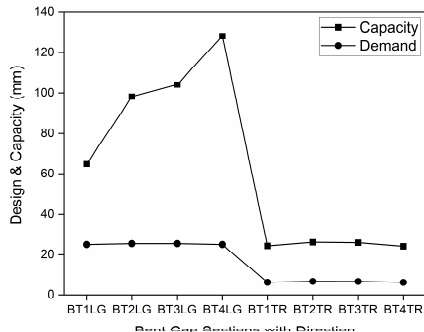


Fig. 6. Demand and capacity of bent cap sections.

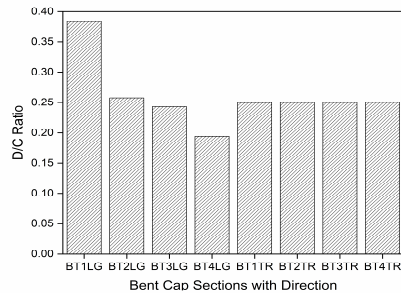


Fig. 7. Demand capacity ratio of bent cap sections.

### C. Drift

To confirm the deformation limit of a bridge structure, Kowalsky, M. J. used the term drift of the structure and a relation with design limit states was established [10]. Drift is the relative displacement of subsequent levels in a structure. Fig. 8, 9, 10 and 11 shows the drifts of all the four piers with respect to pushover loading. In the graphs, B denotes bent cap section and subsequent numbers represent their sequential count. "Long or Trans" represents pushover force in longitudinal or transverse direction. Disp.X and Disp.Y denotes displacement in X and Y directions respectively. Fig. 8 shows the drift of piers in longitudinal direction under the pushover loading in longitudinal direction. Drift of pier 1 due to the base shear force of B1 under pushover loading was found to be 65 mm but under base shear of B2, B3 and B4 drift of pier 1 was 34.5 mm. Among the base shear effects of B1, B2, B3 and B4 on pier 1, effect for B1 was more due to the pushover effect on B1. Drift of pier 1 was double for B1, compared to the base shear effects of four bents. Now in the second part of the graph shows drift of all the piers with respect to the base shear effect of B2 under pushover loading. For B2 base shear, pier 2 drifted 98 mm but for other bent base shears same pier drifted 3 mm only which was 97% less than the effect of B2 base shear under pushover action on pier 2. Bent 2 experienced higher base shear force as we can see from the capacity curve and also bent 2 was having high capacity in longitudinal direction. This is why column 2 was having high drift value in longitudinal direction. In the next part drift of 3<sup>rd</sup> pier was shown with respect to the base shears of four bents.

Drift of 3<sup>rd</sup> pier was found to be 104 mm in the longitudinal direction for base shear force in B3 but for other bent's base shears the pier only drifted 3 mm which also was 97% less than the effect of B3 base shear under pushover action on pier 3. Pier 2 and 3 were supporting similar sections of the bridge and shows similar response against pushover analysis. Last pier drifted 128 mm under the base shear of B4 but under other bent's base shears, the pier drifted nearly 29 mm. 4<sup>th</sup> pier experienced 77% more drift in longitudinal direction under the pushover shear action of B4. Similarly Fig. 9. shows the drift of piers in longitudinal direction under the pushover loading in transverse direction. The figure shows that the pushover force in transverse direction affected all the piers in same way. For all four bent's base shear pier 1 was acting similarly with a drift value of 34.5 mm. similarly 2<sup>nd</sup> and 3<sup>rd</sup> piers were having a drift of 3 mm under the pushover action of all the four bent caps in transverse direction. 4<sup>th</sup> pier showed a drift of 28.7 mm under all base shears of four bents. In transverse direction capacity was same for all the bents leading to same drifts for the piers under pushover loading. From pushover curve we can see that in transverse direction B2 and B3 reached the yield point leading to very less drift in piers.

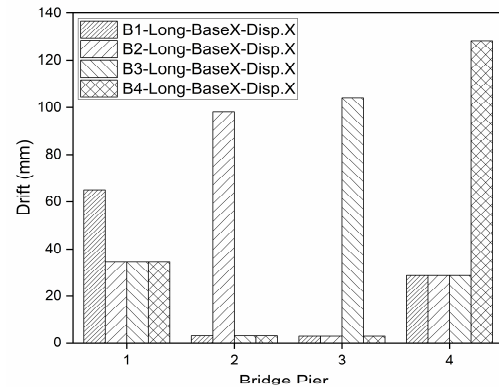


Fig. 8. Drift of columns in longitudinal direction under pushover force in longitudinal direction.

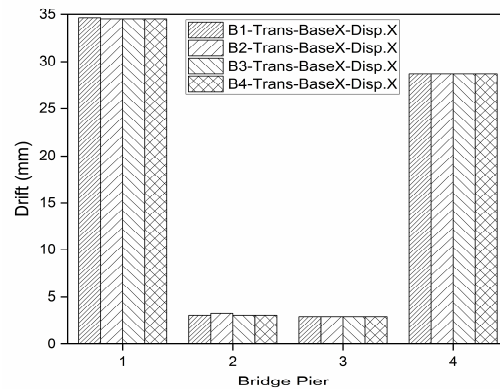
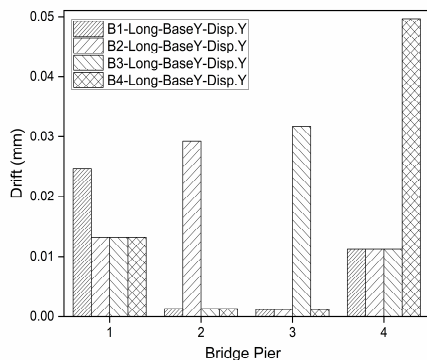


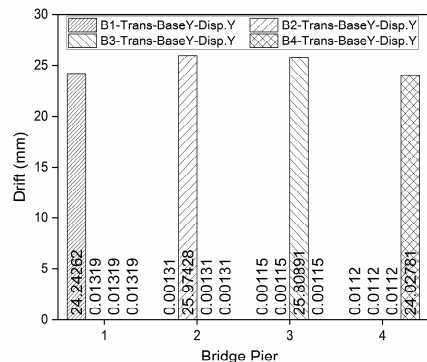
Fig. 9. Drift of columns in longitudinal direction under pushover force in transverse direction.

Fig. 10 shows the drift of piers in transverse direction under the pushover loading in longitudinal direction. The pushover force in longitudinal direction does not have significant effect on the piers in transverse direction. Maximum drift occurred in pier 4 due to the base shear action of B4 which was 0.05 mm. Fig. 11 shows the drift

of piers in transverse direction under the pushover loading in transverse direction. Here peak values were shown in numbers as the peak level was not visible in the graph because of the very low drift value. In this figure, piers were showing similar behaviour like in Fig. 8. Drift of pier 1 due to the base shear force of B1 under pushover loading was found to be 24 mm but under base shear of B2, B3 and B4 drift of pier 1 was 0.011 mm. Among the base shear effects of B1, B2, B3 and B4 on pier 1, effect for B1 was more due to the pushover effect on B1. For B2 and B3 base shears, both pier 2 and 3 drifted 26 mm respectively but for other bent base shears, same pier drifted 0.013 mm only. Pier 2 and 3 were supporting similar sections of the bridge and shows similar response against pushover analysis. Last pier drifted 24 mm under the base shear of B4 but under other bent's base shears, the pier drifted only 0.013 mm.



**Fig. 10.** Drift of columns in transverse direction under pushover force in longitudinal direction.



**Fig. 11.** Drift of columns in transverse direction under pushover force in transverse direction.

## VII. CONCLUSION

A 3D finite element model was analysed for a bridge with self-compacting concrete to evaluate the performance under seismic action. Nonlinear pushover analysis was performed in this order and base shear was analysed under all considered load cases. From the study following points were concluded:

- From base shear study it was found that shear force experienced by the structure was mainly due to the pushover loads. For other load cases negligible base shear reaction was occurred in the bridge.
- In longitudinal direction base shear reached 700 kN but the section did not reached its yield point yet. Whereas in transverse direction base shear was found

to be 4800 kN with reaching the yield point of the section material. This indicates a good capacity of the bridge in both the directions along with most of the displacements were within elastic limit of the structure.

- Maximum demand-capacity (D/C) ratio, considering both the directions, for the bridge structure under study was 0.383, which is within the safety limit value 1.

- Drift study of the columns also showed promising data with higher drift values only in longitudinal direction due to pushover force in that direction. Whereas in transverse direction a negligible drift value of 0.05 mm was observed under the pushover force in longitudinal direction.

- Due to pushover in transverse direction, pier drift in both the direction was very low. Maximum drift in longitudinal and transverse direction was 35 mm and 26 mm respectively, which is in safe limit proving the structure as safe during an earthquake event.

It is concluded that, the bridge was able to resist base shear force during an earthquake event along with a higher base force in the longitudinal direction without reaching the yield point. The design capacity ratio also confirms the safety of the bridge during an earthquake event in the area.

## VIII. FUTURE SCOPE

In this study pushover analysis was carried out on a bridge structure and the performance of the structure was evaluated using self-compacting concrete as construction material. A comparison study is possible on the performance of the bridge using construction materials normal concrete and self-compacting concrete, with the analysis procedure stated above, where ongoing research is undertaken.

**Conflict of Interest.** There is no conflict of interest.

## REFERENCES

- [1]. Lopez, A., Dusicka, P., & Bazaez, R. (2020). Performance of seismically substandard bridge reinforced concrete columns subjected to subduction and crustal earthquakes. *Engineering Structures*, 207, 1–15.
- [2]. Ghosh, G., Singh, Y., & Thakkar, S. K. (2011). Seismic response of a continuous bridge with bearing protection devices. *Engineering Structures*, 33(4), 1149–1156.
- [3]. Kulkarni, R., Adhikary, S., Singh, Y., & Sengupta, A. (2016). Seismic performance of a bridge with tall piers. *Proceedings of the Institution of Civil Engineers: Bridge Engineering*, 169(1), 67 – 75.
- [4]. Priestley, M. J. N., & Seible, F. C. (1996). *Seismic Design and Retrofit of Bridges*. New York, United States of America: John Wiley & Sons.
- [5]. Mohammed, M. S. (2016). *Effect of Earthquake Duration on Reinforced Concrete Bridge Columns*. (Doctoral dissertation, University of Nevada, Reno). Retrieved from ProQuest Dissertations & Theses Global database. (10253151).
- [6]. Feng, Y., Kowalsky, M. J., & Nau, J. M. (2015). Effect of Seismic Load History on Deformation Limit States for Longitudinal Bar Buckling in RC Circular Columns. *Journal of Structural Engineering*, 141(8), 1–13.
- [7]. Goodnight, J. C., Kowalsky, M. J., & Nau, J. M. (2013). Effect of Load History on Performance Limit States of Circular Bridge Columns. *Journal of Bridge Engineering*, 18(12), 1383–1396.
- [8]. Lehman, D., Moehle, J., Mahin, S., Calderone, A., &

- Henry, L. (2004). Experimental evaluation of seismic performance of reinforced concrete bridge columns. *Journal of Structural Engineering*, 869 – 879.
- [9]. Babazadeh, A., Burgueno, R., & Silva, P. F. (2015). Use of 3D Finite-Element Models for Predicting Intermediate Damage Limit States in RC Bridge Columns. *Journal of Structural Engineering*, 141(10), 04015012-1 - 04015012-11.
- [10]. Kowalsky, M. J. (2000). Deformation Limit States for Circular Reinforced Concrete Bridge Columns. *Journal of Structural Engineering*, 126(8), 869–878.
- [11]. Su, J., Dhakal, R. P., & Wang, J. (2017). Fiber-based damage analysis of reinforced concrete bridge piers. *Soil Dynamics and Earthquake Engineering*, 96, 13–34.
- [12]. Meesaraganda, L. V. P., & Tarafder, N. (2019). Durability studies of environmental friendly self compacting concrete with and without fiber. *Key Engineering Materials*, 207–215.
- [13]. Turkel, S., & Kandemir, A. (2010). Fresh and hardened properties of SCC made with different aggregate and mineral admixtures. *Journal of Materials in Civil Engineering*, 22(10), 1025–1032.
- [14]. Public Works Department, Silchar, Assam. Retrived from office.
- [15]. IRC (Indian Road Congress) (2017). *Standard Specifications and Code of Practice for Road Bridges, Section:II, Loads and Load Combinations 7<sup>th</sup> Revision*. IRC-7. New Delhi, India: Indian Road Congress.
- [16]. ACI (American Concrete Institute) (2014). *Building Code Requirements for Structural Concrete*. ACI 318. Michigan, United States of America: American Concrete Institute.
- [17]. IITK-RDSO (Indian Institute of Technology Kanpur-Research Designs and Standards Organisation), (2010). *Guidelines on Seismic Design of Railway Bridges*. NICEE (National Information Centre of Earthquake Engineering), Indian Institute of Technology Kanpur, India: Indian Institute of Technology Kanpur.
- [18]. AASHTO-LRFD (American Association of State Highway and Transportation Officials - Load and Resistance Factor Design) (5<sup>th</sup>), (2010). *Bridge Design Specifications*. New York, United States of America: American Association of State Highway and Transportation Officials.

**How to cite this article:** Tarafder, N. and Prasad, L. V. M. (2020). Seismic Performance of Box Girder Bridge with Non-Linear Static Pushover Analysis. *International Journal on Emerging Technologies*, 11(2): 897–904.